April, 1993

Independent Modes of Propagation of Calcium Waves in Smooth Muscle Cells

David Gross, *University of Massachusetts - Amherst*
P. K Hepler
L. L Slakey
M. G Mahoney

Journal of Cell Science 104, 1101-1107 (1993)
Printed in Great Britain © The Company of Biologists Limited 1993

Independent modes of propagation of calcium waves in smooth muscle cells

Mỹ G. Mahoney[1,*], Linda L. Slakey[1], Peter K. Hepler[2] and David J. Gross[1]

[1]Program in Molecular and Cellular Biology and Department of Biochemistry and Molecular Biology
[2]Department of Botany, University of Massachusetts, Amherst, MA 01003, USA

*Author for correspondence

SUMMARY

The purinergic agonist adenosine triphosphate (ATP) stimulates an initial transient followed by subsequent oscillations in cytosolic calcium ion concentration ($[Ca^{2+}]_i$) in individual porcine aortic smooth muscle cells. Using microinjection of fura-2 covalently coupled to dextran, we have analyzed in detail the spatial and temporal features of the oscillations. We have observed both cytoplasmic calcium waves and gradients within single cells. Single cells can contain multiple loci of initiation of oscillations. Independent oscillations in a single cell can have independent frequencies and these oscillations can propagate without interference across the same region of the cell, suggesting that they arise either from separately regulated stores of Ca^{2+} or a single Ca^{2+} store operated by two separate release mechanisms. The shape of the wave front and the manner of the wave's decay can vary from one oscillation to the next. Ca^{2+} signaling in individual arterial smooth muscle cells thus displays complex spatial and temporal organization.

Key words: ATP, purinergic receptors, Ca^{2+} signaling, fura-2 dextran, smooth muscle

INTRODUCTION

Stimulation with extracellular ATP induces a nucleotide receptor-mediated rapid initial transient rise followed by asynchronous periodic oscillations of cytosolic Ca^{2+} activity ($[Ca^{2+}]_i$) in individual porcine aortic smooth muscle cells (Linderman et al., 1990; Mahoney et al., 1992). Because $[Ca^{2+}]_i$ is the primary regulator of excitation-contraction coupling in smooth muscle cells (Somlyo and Himpens, 1989), it is clear that spatiotemporal regulation of the $[Ca^{2+}]_i$ responses is critical in the regulation of the contractile state of individual smooth muscle cells within a tissue.

Since the first report that $[Ca^{2+}]_i$ signals propagate as waves in oocytes (Gilkey et al., 1978), it has become increasingly clear that calcium second messenger signaling has both a temporal and spatial component. Receptor-mediated $[Ca^{2+}]_i$ waves have been reported in glutamate-stimulated astrocytes (Cornell-Bell et al., 1990), vasopressin-stimulated hepatocytes (Rooney et al., 1990), and vasopressin-stimulated A7r5 cultured vascular smooth muscle cells (Wier and Blatter, 1991), among others. This subject has been recently reviewed by Meyer (1991) and Jaffe (1991).

Meyer notes that two essential aspects of $[Ca^{2+}]_i$ waves in cells are diffusion of Ca^{2+} and positive feedback in the amplification cascade leading to $[Ca^{2+}]_i$ elevation. Models in the literature that have been applied to $[Ca^{2+}]_i$ wave signaling include the $[Ca^{2+}]_i$ amplification of phospholipase C (PLC) model of Meyer and Stryer (Meyer, 1991; Meyer and Stryer, 1988), the calcium-induced calcium release (CICR) model by Dupont et al. (1991), and models incorporating feedback due to protein kinase C (Cuthbertson and Chay, 1991). In the first model, a ligand-bound receptor activates a GTP-binding protein (G-protein) that, in turn, activates PLC. This PLC activity hydrolyzes phosphatidylinositol (PIP_2) to form inositol 1,4,5-trisphosphate (IP_3) that releases Ca^{2+} from IP_3-sensitive Ca^{2+} stores. The initial elevation of $[Ca^{2+}]_i$ stimulates further IP_3 production by positive feedback on PLC. The second model, CICR, proposes that Ca^{2+} is first released from an IP_3-sensitive pool and, in the continued presence of IP_3, is taken up into an IP_3-insensitive pool. Overloading the IP_3-insensitive pool or elevation of cytoplasmic $[Ca^{2+}]$ triggers release of Ca^{2+} from this pool into the cytoplasm. The third model involves oscillations of $[IP_3]$ and $[Ca^{2+}]_i$ through both negative feedback from protein kinase C (PKC) onto G-proteins and also receptors, and positive feedback of Ca^{2+} onto PLC.

It has been recently reported that *Xenopus* oocytes, expressing muscarinic acetylcholine receptors, respond to acetylcholine stimulus with propagating circular and spiral $[Ca^{2+}]_i$ waves (Lechleiter et al., 1991). These waves originate from separate foci in the ooplasm and have been shown to propagate by a modified CICR mechanism in which ele-

vated $[Ca^{2+}]_i$ enhances release from IP_3-sensitive calcium stores which, subsequent to Ca^{2+} release, become refractory (Delisle and Welsh, 1992; Lechleiter and Clapham, 1992).

In this report, we describe two types of $[Ca^{2+}]_i$ spatial signals in ATP-stimulated pig aortic smooth muscle cells: propagating waves and transient gradients. Individual smooth muscle cells were microinjected with the Ca^{2+} indicator fura-2 covalently coupled to dextran (fura-dextran). Cytosolic fura-dextran cannot be compartmentalized into organelles or extruded from the cells (Miller et al., 1992), in contrast to the acetoxymethyl ester or free anion form of the dye (Moore et al., 1990; Roe et al., 1990); this allows measurement of $[Ca^{2+}]_i$ in the cytosol with no contribution from organelle-sequestered dye and without reliance on cellular esterase activity. The $[Ca^{2+}]_i$ waves we describe are novel in that different regions of initiation of the waves are found in a single cell and that multiple independent oscillators are found in a single cell. We present evidence that different modes of oscillation are mediated by different mechanisms.

MATERIALS AND METHODS

Cell culture

Vascular smooth muscle cells were isolated from medial tissue of swine aorta as described previously (Goldman et al., 1983). For experiments, subcultured cells from passages 3-15 were grown overnight on no.1 glass coverslips in 35 cm^2 culture dishes in a growth medium consisting of DMEM (Dulbecco's modified Eagle's medium; Gibco, Grand Island, NY) supplemented with 200 i.u./ml penicillin, 0.2 mg/ml streptomycin and 10% fetal calf serum, and thereafter in defined medium (DMEM supplemented with 5.0 μg/ml transferrin, 6.0 μg/ml insulin and 0.04 mg/ml ascorbic acid). Experiments were performed approximately 96 hours after plating onto coverslips.

fura-2/AM or fura-dextran loading and $[Ca^{2+}]_i$ imaging

For fura-dextran loading, the cells were quickly rinsed in HEPES-buffered saline (HBS is, in mM, 20 HEPES (pH 7.4), 125 NaCl, 5.4 KCl, 1.8 $CaCl_2$, 0.8 $MgSO_4$, 5.5 D-glucose), pressure injected with 20 mg/ml fura-dextran (10 kDa; Molecular Probes, Inc., Eugene, OR) in 100 mM KCl, and returned to defined medium for 30 min at 37°C in a 95% air/5% CO_2 atmosphere to allow the dye to distribute homogeneously throughout the cell. For fura-2/AM loading, the cells were incubated with 2 μM fura-2/AM (from a 1 mM stock in DMSO; Molecular Probes, Inc., Eugene, OR) for 30 min at 37°C in a 95% air/5% CO_2 atmosphere. The coverslip was then washed with HBS and mounted in a flow chamber held at 37°C in HBS on a Zeiss IM-35 microscope (Carl Zeiss, Inc., Thornwood, NY) in HBS. Extracellular ATP was perfused in HBS. Fluorescence images of the cells were acquired by a charge-coupled device (CCD) instrumentation camera (Photometrics, Ltd., Tucson, AZ) as previously described (Linderman et al., 1990). Images were captured by illumination at 365 nm and 334 nm with typical exposure times of 25 and 250 ms, respectively.

Extracellular ATP in HBS was perfused into the cell chamber as previously described (Linderman et al., 1990; Cheyette and Gross, 1991). Cheyette and Gross showed that the complete exchange of fluid in the cell chamber took approximately 2 s.

$[Ca^{2+}]_i$ calibration

Using a blank-field background image void of cells, ratio ($R=(F_{334}-F_{334(blank)})/(F_{365}-F_{365(blank)})$) images were generated and pCa images were computed using calibration images with minor changes in the procedure described previously (Linderman et al., 1990). Briefly, fluorescence images of 0.3 ml of fura-dextran (40 μg/ml) or fura-2 free acid (10 μM) in a HEPES buffer (pH 7.4) containing 10 mM HEPES, 150 mM KCl, 0.2 % NaN_3 supplemented with 5 mM EGTA or 500 μM $CaCl_2$, or buffer alone (for background subtraction), were collected. Using these images, R_{max}, R_{min} and β were calculated: $R_{max} = (F_{334}/F_{365})$ at saturating Ca^{2+}, $R_{min} = (F_{334}/F_{365})$ at no Ca^{2+}, and $\beta = F_{365}$(no Ca^{2+})/F_{365}(saturating Ca^{2+}). The formula $[Ca^{2+}]_i = K_d\beta[(R-R_{min})/(R_{max}-R)]$, where K_d = 394 nM is the equilibrium dissociation constant for Ca^{2+} and fura-dextran was used to compute $[Ca^{2+}]_i$. Calibration corrections for high intracellular viscosity were measured in solutions containing 60% (w/v) sucrose (Poenie, 1990), as described previously (Linderman et al., 1990). Resting $[Ca^{2+}]_i$ levels calculated using these calibration images were ~60 to 140 nM.

Calibrations for fura-2/AM-loaded cells were done by computation from ratio values as described previously (Mahoney et al., 1992). The initial resting ratio value was set to pCa = 7 and $[Ca^{2+}]_i$ calculated from the antilog of the normalized ratio value.

Replication

Illustrative results are presented in the figures for 2 individual cells. Twenty two cells, 10 injected with fura-dextran and 12 loaded with fura-2/AM were examined for the presence of Ca^{2+} waves and gradients. Data from all cells were included in the computation of average wave speed and gradient.

RESULTS

We have recently shown that pig arterial smooth muscle cells respond to extracellular ATP stimulation with an initial transient rise followed by oscillations of $[Ca^{2+}]_i$ that are asynchronous from cell to cell. Individual cells display differences in the details of this response in a dose-dependent manner, but more than 90% of the cells respond in this fashion with 50 μM ATP stimulation (Mahoney et al., 1992). In the experiments reported here, single arterial smooth muscle cells were loaded with fura-dextran by microinjection. In all 10 cells examined by this method, waves and gradients of $[Ca^{2+}]_i$ were found. Representative results from two of these cells are described below.

Spatial inhomogeneity of initial transient

In response to 50 μM ATP, $[Ca^{2+}]_i$ averaged over a whole cell increased from ~140 nM to ~10 μM within 4 s of stimulus (Fig. 1A). Fig. 1B shows the rise and decline of the initial transient in three regions of the cell (see inset of Fig. 1A). The $[Ca^{2+}]_i$ increase in all three regions is first detected in the image captured 4 s after stimulation. Both at 4 s and at peak, the right region (■) attained a higher $[Ca^{2+}]_i$ than the center (Δ) or left region (●). Although $[Ca^{2+}]_i$ was changing rapidly during these time points, all portions of the cell were sampled in parallel, thus, the relative differences in $[Ca^{2+}]_i$ in different parts of the cell can be compared. The fact that a measured $[Ca^{2+}]_i$ gradient was present at both time points supports the notion that a real

gradient was present. During the declining phase of the initial transient, $[Ca^{2+}]_i$ in the right region dropped below that in regions a and b until $[Ca^{2+}]_i$ reached ~200 nM, at which point this condition reversed. Thus, in this cell, a $[Ca^{2+}]_i$ gradient from right to left was established during the rising phase of the response, it reversed transiently during the decline, and finally reversed again as $[Ca^{2+}]_i$ approached pre-stimulus levels. In all 10 ATP-stimulated arterial smooth muscle cells observed using fura-dextran, the initial $[Ca^{2+}]_i$ rise began in a peripheral region of a cell and migrated away from the initiation point across the cell in a manner similar to that displayed in the cell of Fig. 1. This result contrasts with that of Wier and Blatter (1991) in which vasopressin stimulation of A7r5 cultured vascular smooth muscle cells produced an initial $[Ca^{2+}]_i$ rise at the cell perimeter that propagated inward toward the cell center.

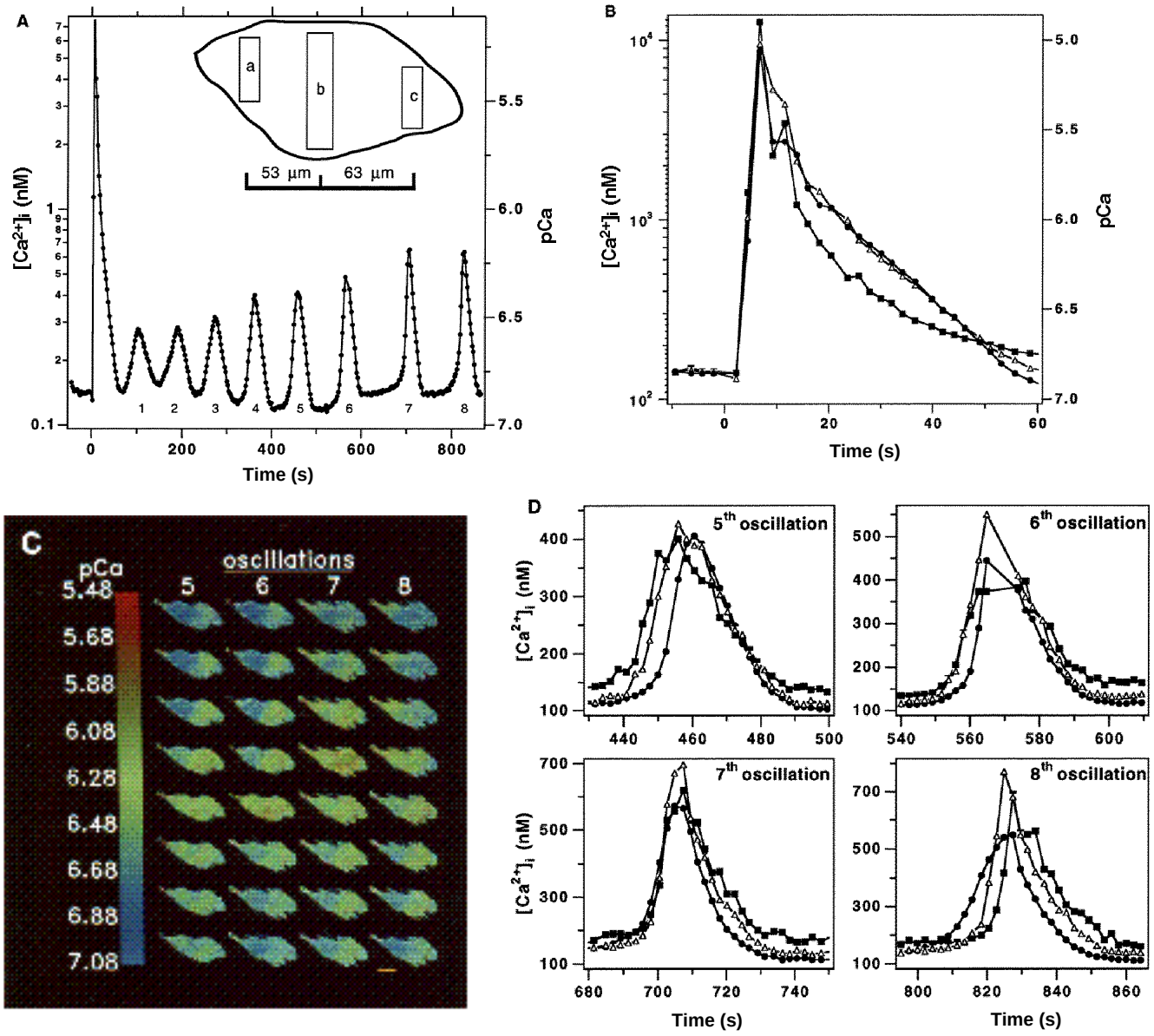

Fig. 1. Pseudocolor fluorescence images of a single porcine aortic smooth muscle cell stimulated with ATP and plots of cytoplasmic calcium concentration show differential spatiotemporal distribution of $[Ca^{2+}]_i$. (A) $[Ca^{2+}]_i$ averaged over the whole cell shows one initial transient rise followed by 8 oscillatory spikes of $[Ca^{2+}]_i$ (labelled 1 through 8) in the continuous presence of ATP during the 15 min duration of this experiment. Inset: schematic diagram of the cell and the regions a, b and c. (B) $[Ca^{2+}]_i$ measured in regions a (●), b (Δ) and c (■) of the cell during the initial transient. (C) fura-dextran $[Ca^{2+}]_i$ images of the cell during: (1) the 5th oscillation at 443, 445, 448, 452, 456, 470, 472 and 475 s after stimulation with 50 µM ATP, (2) the 6th oscillation at 554, 556, 558, 560, 565, 583, 586 and 588 s subsequent to ATP addition, (3) the 7th oscillation at 696, 698, 700, 703, 716, 718, 720, and 722 s subsequent to ATP addition, and (4) the 8th oscillation at 813, 816, 818, 820, 838, 841, 843 and 854 s subsequent to ATP addition. Time increases from top to bottom in each column. Bar, 50 µm. A color scale map from 84 to 3300 nM $[Ca^{2+}]_i$ is shown to the left. (D) $[Ca^{2+}]_i$ measured over regions a (●), b (Δ) and c (■) during the 5th through 8th oscillations.

ATP-stimulated $[Ca^{2+}]_i$ oscillations with multiple initiation sites

As $[Ca^{2+}]_i$ returned to near baseline after the initial transient, oscillations began (Fig. 1A). We have previously shown that ATP-stimulated oscillations in these cells arise from intracellular stores of calcium (Mahoney et al., 1992) although extracellular Ca^{2+} is required to replenish the stores. ATP-stimulated $[Ca^{2+}]_i$ oscillations showed substantial variability in the spatial disposition of their initiation and decay (Fig. 1C). The first six oscillations initiated in the right region of the cell while the 8th oscillation initiated from the left region of the cell. The 7th oscillation simultaneously initiated from both loci. In this intermediate, 7th oscillation, the average peak $[Ca^{2+}]_i$ was only slightly higher than that of the previous (6th) oscillation (Fig. 1A), indicating that $[Ca^{2+}]_i$ elevation resulting from the combination of the two independently initiated waves was not additive. The first five oscillations decayed homogeneously across the cell. Beginning with the 6th oscillation, however, the decay of each oscillation developed an increasingly pronounced spatial gradient, with $[Ca^{2+}]_i$ in the right region of the cell returning to baseline after that in the left side. The 6th oscillation rises from and returns to the same region of the cell. We refer to this as a pulsing gradient. The 8th oscillation clearly represents a propagating wave traveling from one side of the cell to the other. Thus, the mode of $[Ca^{2+}]_i$ propagation during this series of oscillations changed from a pulsing gradient to a propagating wave concomitant with the shift in the locus of initiation of the $[Ca^{2+}]_i$ transient.

Multiple oscillation frequencies within an individual ATP-stimulated cell

A second level of complexity in $[Ca^{2+}]_i$ signaling in smooth muscle cells was demonstrated in the cell shown in Fig. 2. When $[Ca^{2+}]_i$ was averaged over the whole cell, only 4 clear oscillations were observed (Fig. 2A). However, the bottom region of the cell (region d) displayed six separate oscillations, while other regions of the cell displayed only four (Fig. 2B). The four oscillations in regions a, b and c propagated into region d as shown by the time delay of the arrival of peak $[Ca^{2+}]_i$ (Fig. 2B). Two distinct sets of oscillations were seen in region d as is shown in Fig. 2C. In this figure, the same lines of pixels along the axis of the cell were sampled for each of the 200 images in the 600 s time-lapse sequence, and the lines from each image were

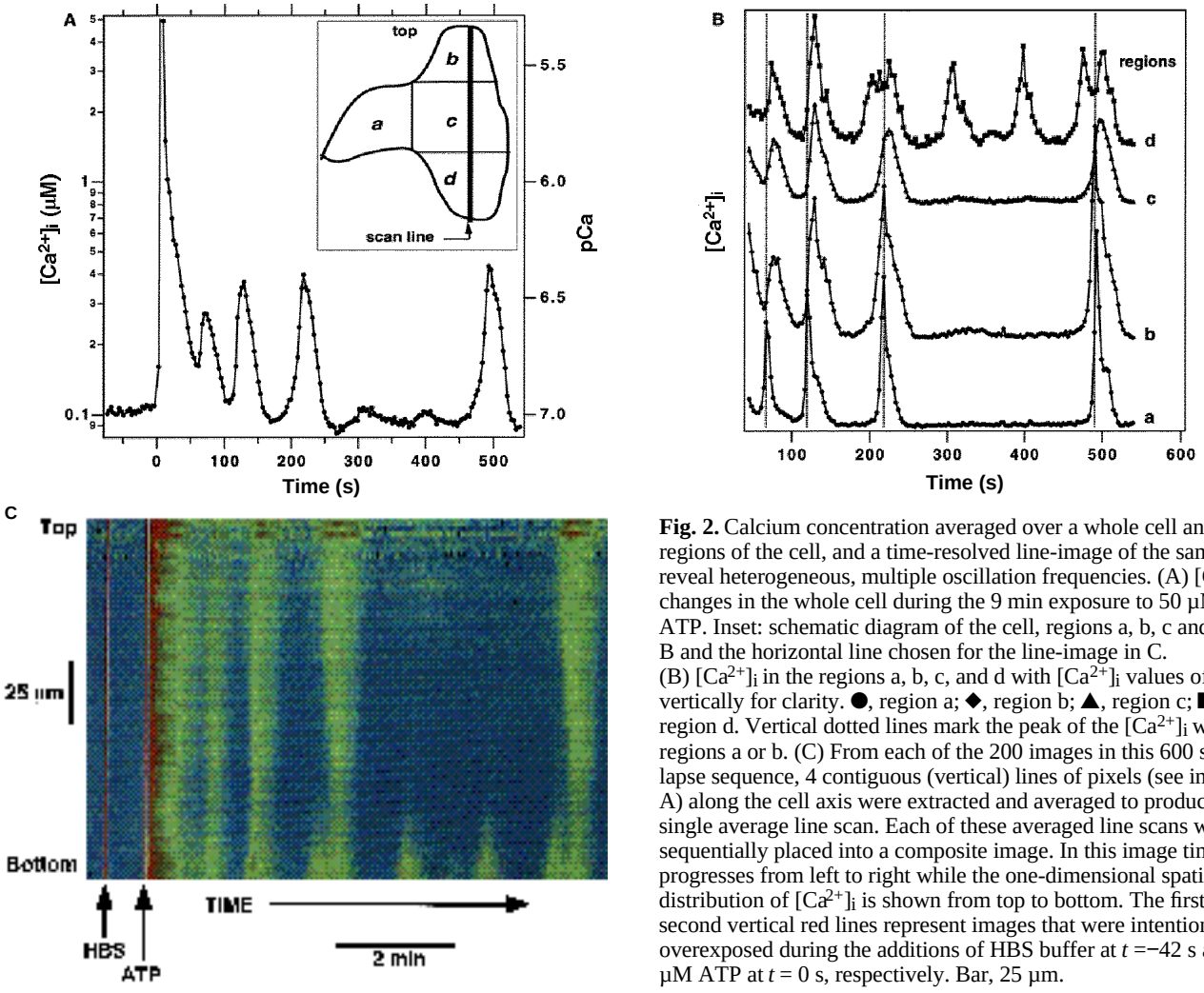

Fig. 2. Calcium concentration averaged over a whole cell and regions of the cell, and a time-resolved line-image of the same cell reveal heterogeneous, multiple oscillation frequencies. (A) $[Ca^{2+}]_i$ changes in the whole cell during the 9 min exposure to 50 μM ATP. Inset: schematic diagram of the cell, regions a, b, c and d for B and the horizontal line chosen for the line-image in C. (B) $[Ca^{2+}]_i$ in the regions a, b, c, and d with $[Ca^{2+}]_i$ values offset vertically for clarity. ●, region a; ◆, region b; ▲, region c; ■, region d. Vertical dotted lines mark the peak of the $[Ca^{2+}]_i$ wave in regions a or b. (C) From each of the 200 images in this 600 s time-lapse sequence, 4 contiguous (vertical) lines of pixels (see inset in A) along the cell axis were extracted and averaged to produce a single average line scan. Each of these averaged line scans was sequentially placed into a composite image. In this image time progresses from left to right while the one-dimensional spatial distribution of $[Ca^{2+}]_i$ is shown from top to bottom. The first and second vertical red lines represent images that were intentionally overexposed during the additions of HBS buffer at $t = -42$ s and 50 μM ATP at $t = 0$ s, respectively. Bar, 25 μm.

arranged horizontally in sequence to produce a one spatial dimension (vertical direction) versus time (horizontal direction) image. The bottom of Fig. 2C (region d in Fig. 2A,B) shows two independent sets of oscillations, one of which propagated into region d from region c and one of which was localized to region d only.

Wave speeds and magnitude of gradients

To quantitate the magnitude and rate of the $[Ca^{2+}]_i$ wave and gradient propagations during these oscillations, $[Ca^{2+}]_i$ was measured in the three regions of the cell shown in the inset of Fig. 1A. Plots of the $[Ca^{2+}]_i$ oscillations versus time in these three subregions for the 5th through the 8th oscillations demonstrate that the initiation site of the oscillations changes over time and that the mode of propagation (wave versus gradient) of the $[Ca^{2+}]_i$ signal changes from oscillation to oscillation (Fig. 1D).

The average speeds of the $[Ca^{2+}]_i$ wave fronts during the rising phase of the 1st through the 6th oscillations were, respectively, 4.2, 2.8, 4.7, 5.9, 8.1 and 8.6 μm/s. Wave speeds were determined from plots of $[Ca^{2+}]_i$ versus position along the direction of wave propagation for time points during the rising phase of each oscillation as shown in Fig. 3 for the 3rd and 5th oscillations. The location of the wave front for which $[Ca^{2+}]_i$ = 200 nM was chosen as the position of the wave at each time point. For the 5th oscillation (Fig. 3B), wave speed was nearly constant as the wave traversed the cell; however, in the 3rd oscillation (Fig. 3A), wave speed increased as the wave traversed the cell. Oscillations began with a shallow gradient that increased in steepness with time. Once a $[Ca^{2+}]_i$ gradient became established at the leading edge of a wave, its steepness (change of $[Ca^{2+}]_i$ over distance as in Fig. 3A,B) remained relatively constant across the cell, indicating that the $[Ca^{2+}]_i$ flux at the leading edge of a wave is approximately constant. The steepness of the $[Ca^{2+}]_i$ wave front, and thus the Ca^{2+} flux, varied from oscillation to oscillation (Fig. 3A,B). An anomalous $[Ca^{2+}]_i$ elevation at 50 μm from the left side of the cell was seen during each oscillation as the wave front passed this point, suggesting that this may be a region of the cell in which calcium release from internal stores is greatest.

Cells microinjected with fura-dextran or loaded with fura-2 by incubation with its acetoxymethyl ester (fura-2/AM) were carefully examined for such spatial $[Ca^{2+}]_i$ inhomogeneities. The average wave speed and gradient steepness of each oscillation in 10 fura-dextran- and 12 fura-2/AM-loaded cells were determined. All 22 cells show $[Ca^{2+}]_i$ gradients. $[Ca^{2+}]_i$ spread at an average speed of 3.9 ± 1.2 μm/s for fura-dextran-loaded cells while the speed is significantly faster, 6.5 ± 2.4 μm/s, with fura-2/AM-loaded cells (Student's *t*-test, $P < 0.005$). Although the $[Ca^{2+}]_i$ gradient steepness was slightly less in fura-2/AM-loaded cells (3.8 ± 2.4 nM/μm) versus fura-dextran-loaded cells (4.7 ± 1.8 nM/μm), the difference was not statistically significant (Student's *t*-test, $P > 0.1$).

In fura-dextran-loaded cells, all injections were aimed towards the center of the cell where the height of the cell is greatest, while $[Ca^{2+}]_i$ gradients typically started at the periphery. Also, there was no correlation between the injection sites and local regions of high basal $[Ca^{2+}]_i$. $[Ca^{2+}]_i$ oscillations and the direction of the propagating waves in any particular cell did not correlate with $[Ca^{2+}]_i$ signals in neighboring cells. In all ATP-stimulated cells, whether loaded with fura-dextran or fura-2/AM, multiple sites of initiation and modes of propagation of $[Ca^{2+}]_i$ gradients were found similar to those shown here.

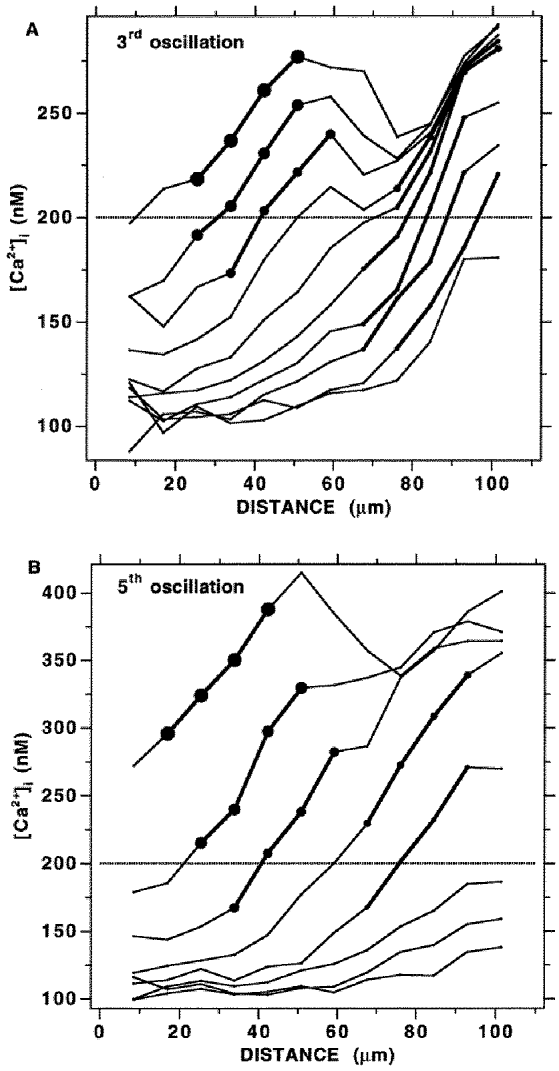

Fig. 3. $[Ca^{2+}]_i$ gradients at different times in the cell of Fig. 1 reveal relatively constant $[Ca^{2+}]_i$ fluxes at the propagating wave fronts. The $[Ca^{2+}]_i$ in twelve regions 8.45 μm wide by 19 μm high in a horizontal row across the center of the cell of Fig. 1 was examined at several time points. (A) *t* = 248, 250, 252, 254, 256, 259, 262, 264, 266, 268 s during the 3rd oscillation. (B) *t* = 438, 441, 443, 445, 448, 450, 452 and 454 s during the 5th oscillation. Increasing time points are indicated by increasingly large ● symbols. The phase of the gradient that rises most steeply is shown in bold. Slopes of the steepest part of the gradient were computed for each time point in which a $[Ca^{2+}]_i$ greater than 100 nM above the basal $[Ca^{2+}]_i$ was observed. The steepness was computed from the four contiguous points that yielded the greatest slope. The slopes of the bold portions of each trace are, in ascending order, 1.9, 2.5, 2.2, 2.4, 2.3, 3.0, 3.9, 3.3, 2.9 nM/μm for the 3rd oscillation and 4.1, 4.2, 4.0, 3.3 and 3.4 nM/μm for the 5th oscillation.

DISCUSSION

We have previously shown that pig arterial smooth muscle cells respond to nucleotide receptor stimulus by ATP with an initial transient rise in $[Ca^{2+}]_i$ that decays over time and that is followed by persistent oscillations of $[Ca^{2+}]_i$ (Mahoney et al., 1992). Both the initial transient and oscillations are produced by ligand-activated Ca^{2+} release from intracellular stores, although the initial transient is prolonged in Ca^{2+}-containing medium as compared to Ca^{2+}-free medium and the oscillations are not established in the absence of external Ca^{2+}. It appears that intracellular Ca^{2+} store refilling is necessary for oscillations to persist. In this report we show that there are two types of nucleotide receptor-mediated $[Ca^{2+}]_i$ spatial signals, one a gradient, similar to the $[Ca^{2+}]_i$ gradients observed in hepatocytes (Rooney et al., 1990), and the other a propagating wave, similar to those observed in cardiac cells (Takamatsu and Wier, 1990). We further show that independent sites of initiation of the $[Ca^{2+}]_i$ waves and gradients exist in an individual cell, and that these sites can act independently of each other. Within the time resolution of observation of change in $[Ca^{2+}]_i$, the nucleotide stimulant was applied uniformly across the surface of the plasma membrane (Materials and Methods). Therefore, spatial control of $[Ca^{2+}]_i$ transients must arise from the intrinsic properties of the cell itself. Receptors, receptor-activated enzymes, intracellular Ca^{2+} stores or other components of the Ca^{2+}-second messenger signaling cascade could be concentrated within subregions of cells, thus allowing spatial regulation of the $[Ca^{2+}]_i$ response.

The presence of two independent sets of $[Ca^{2+}]_i$ oscillations in one region (d) of the cell shown in Fig. 2 provides insight into the nature of the mechanism of $[Ca^{2+}]_i$ propagation in arterial smooth muscle cells. Fig. 2C shows that the $[Ca^{2+}]_i$ oscillation localized to region d of the cell (referred to below as the local oscillator) does not propagate more than 30 μm away from that region while an independent wave (referred to below as the global oscillator) initiating from region b propagates across the whole cell into region d. Further, in region d, the inability of the rise and subsequent fall of $[Ca^{2+}]_i$ due to the local oscillation to block the incoming propagation of the oscillation originating in region b (Fig. 2B) shows that calcium stores from which the propagating oscillations arise are either independent of those of the local oscillation or they are neither depleted nor desensitized by the local oscillation.

The data indicate that at most one of the oscillators (global or local) could be due to the proposed calcium-induced calcium release model of $[Ca^{2+}]_i$ waves (Dupont et al., 1991), since in this model elevated Ca^{2+} is a positive feedback element. If the global oscillator is controlled by CICR, then the local oscillator cannot be because it would also produce a wave that propagates across the cell. If the local oscillator is controlled by CICR, obviously only a localized pool of Ca^{2+} is sensitive to this mechanism. An analogous argument can be made for the model in which Ca^{2+}-positive feedback of IP_3-mediated Ca^{2+} release produces self-regenerative $[Ca^{2+}]_i$ waves in *Xenopus* oocytes (Girard et al., 1992), and for the model of $[Ca^{2+}]_i$ oscillations in which IP_3 levels oscillate and $[Ca^{2+}]_i$ exerts positive feedback on its own release and on IP_3 production (Harootunian et al., 1991). By analogous argument we mean that at most one of the oscillators can be explained by the model in question and if it is the local oscillator the relevant pool is spatially limited. No two of the above three models could be present simultaneously, because all contain elevated Ca^{2+} as a positive feedback element. Even though one model also contains an independently necessary element, in any combination of two of them, propagation of both would occur simultaneously.

Similarly, the observation of both pulsing gradients and propagating waves in the same cell (Fig. 1) implies that there are at least two mechanisms of control of $[Ca^{2+}]_i$ in these cells. The observation of a pulsing gradient implies at least either a localized pool of Ca^{2+} accessible to that mechanism for release, or non-uniform spatial distribution of reuptake. On the other hand, to sustain a propagating wave there must be a globally accessible release pool coupled with uniform distribution of Ca^{2+} removal sites.

A hypothesis that can explain this phenomenon is that the two spatially separate loci of origin of the $[Ca^{2+}]_i$ oscillations are responding to two different Ca^{2+} releasing agents and that one of these releasing agents produces a propagating $[Ca^{2+}]_i$ wave. IP_3 and cyclic ADP-ribose are two putative independent Ca^{2+}-releasing agents as they have been shown to act independently to release Ca^{2+} (Dargie et al., 1990). If two different Ca^{2+}-releasing agents are acting in the cell of Fig. 2, then the one responsible for the local oscillator must be incapable of Ca^{2+} release beyond the locale of that oscillator. This could be accomplished by localized production of the releasing agent, perhaps coupled with rapid degradation of the releasing agent, or by localization of the Ca^{2+} stores sensitive to that agent.

Our data can be used to estimate the magnitude of the Ca^{2+} flux occurring during $[Ca^{2+}]_i$ waves. The mean spatial gradient of $[Ca^{2+}]_i$ in propagating waves measured as described in the legend of Fig. 3, 4.7 nM/μm, can be used to calculate the mean calcium ion flux (obtained from Fick's law: $J_{Ca} = -D_{Ca}(\partial[Ca^{2+}]_i/\partial x)$ with $D_{Ca} = 4 \times 10^{-6}$ cm^2/s (Kargacin and Fay, 1991), where we consider only the Ca^{2+} flux in the plane of the specimen). The flux calculated is 1.8×10^{-21} mol/μm^2 s = 1100 Ca ions/μm^2 s in the direction of movement of the wave. This flux is a lower-limit estimate of the true calcium ion flux, since the presence of mobile cytosolic buffers will mask some of the moving Ca^{2+}.

The fact that the leading edges of the $[Ca^{2+}]_i$ waves in these cells move with an average speed of 4 μm/s in furadextran-loaded cells raises the question of blurring of the edge of the wave during the time of image exposure. All of the data shown here were collected with exposure time of 25 ms at 334 nm excitation and 250 ms at 365 nm excitation. The start of the second exposure was delayed 300 ms after the end of the first exposure, so that one complete image set was collected in 575 ms. On average, a $[Ca^{2+}]_i$ wave front would have moved 2.3 μm in that time. This value represents the limiting distance over which the wave front is resolved. The data shown here were collected by combining 4 pixels in both the *x* and *y* directions on the CCD (Linderman et al., 1990) for a spatial resolution of 2.1 μm. Thus for our data, blurring during the wave movement is not significant.

The attenuation of measured spatial $[Ca^{2+}]_i$ inhomogeneity in fura-2/AM-loaded cells compared to fura-dextran-loaded cells may result from the incorporation of fura-2 into organelles or the relatively higher mobility of fura-2 in the cytosol. The former would tend to mask cytosolic $[Ca^{2+}]$ changes while the latter would tend to dissipate $[Ca^{2+}]_i$ gradients by shuttle-buffer effects (Speksnijder et al., 1989). As discussed by Sala and Hernandez-Cruz (1990), the effect of increased mobility of a Ca^{2+} buffer is to increase the rate at which $[Ca^{2+}]_i$ gradients dissipate, i.e. to increase the effective diffusion coefficient for Ca^{2+}. Allbritton et al. (1992) have shown that the diffusion of Ca^{2+} in *Xenopus* oocyte cytoplasmic extract is attenuated by immobile Ca^{2+} buffers. As noted by Meyer (1991), the velocity of $[Ca^{2+}]_i$ wave propagation increases as $D_{Ca}^{\frac{1}{2}}$; thus our finding that $[Ca^{2+}]_i$ wave speeds are greater in the presence of fura-2 free acid than fura-dextran is consistent with the idea that the free acid is facilitating diffusion of Ca^{2+} in the cell.

Arterial smooth muscle cells display two unique features in the propagation of agonist-stimulated $[Ca^{2+}]_i$ oscillations, compared to the traveling waves and spatial gradients of $[Ca^{2+}]_i$ in agonist-stimulated individual cells that have been previously reported (Cornell-Bell et al., 1990; Rooney et al., 1990; Lechleiter et al., 1991; Wier and Blatter, 1991). First, these cells produce oscillations that initiate from different loci within the cell. Second, separate regions within a single cell can sustain independent $[Ca^{2+}]_i$ oscillations that arise from separate loci within the cell. These localized $[Ca^{2+}]_i$ transients may be employed by the cell to spatially and temporally regulate $[Ca^{2+}]_i$-dependent enzymes to effect localized control over enzyme activity.

We thank Dale A. Callaham for introducing us to fura-dextran and microinjection. We thank Clare Fewtrell, Edward W. Westhead and Lionel F. Jaffe for critically reading the original manuscript and particularly the Journal of Cell Science reviewer for very helpful comments. This work was supported by the National Institutes of Health (HL 31854), and the National Science Foundation (DCB-9105429 and DCB-9004191).

REFERENCES

Allbritton, N. L., Meyer, T. and Stryer, L. (1992). Range of messenger action of calcium ion and inositol 1,4,5-trisphosphate. *Science* **258**, 1812-1815.

Cheyette, T. E. and Gross, D. J. (1991). Epidermal growth factor-stimulated calcium ion transients in individual A431 cells: Initiation kinetics and ligand concentration dependence. *Cell Regul.* **2**, 827-840.

Cornell-Bell, A. H., Finkbeiner, S., Cooper, M. S. and Smith, S. J. (1990). Glutamate induces calcium waves in cultured astrocytes: long-range glial signaling. *Science* **247**, 470-473.

Cuthbertson, K. S. R. and Chay, T. R. (1991). Modeling receptor-controlled intracellular Ca^{2+} oscillations. *Cell Calcium* **12**, 97-109.

Dargie, P. J., Agre, M. C. and Lee, H. C. (1990). Comparison of Ca^{2+} mobilizing activities of cyclic ADP-ribose and inositol trisphosphate. *Cell Regul.* **1**, 279-290.

Delisle, S. and Welsh, M. J. (1992). Inositol trisphosphate is required for the propagation of calcium waves in Xenopus oocytes. *J. Biol. Chem.* **267**, 7963-7966.

Dupont, G., Berridge, M. J. and Goldbeter, A. (1991). Signal-induced Ca^{2+} oscillations: properties of a model based on Ca^{2+}-induced Ca^{2+} release. *Cell Calcium* **12**, 73-85.

Gilkey, J. C., Jaffe, L. F., Ridgway, E. B. and Reynolds, G. T. (1978). A free calcium wave traverses the activating egg of the medaka. *J. Cell Biol.* **76**, 448-466.

Girard, S., Luckhoff, A., Lechleiter, J., Sneyd, J. and Clapham, D. (1992). Two-dimensional model of calcium waves reproduces the patterns observed in Xenopus oocytes. *Biophys. J.* **61**, 509-517.

Goldman, S. J., Dickinson, E. S. and Slakey, L. L. (1983). Effects of adenosine on synthesis and release of cyclic AMP by cultured vascular smooth muscle cells from swine. *J. Cyclic Nucleotide Res.* **9**, 69-78.

Harootunian, A. T., Kao, J. P. Y., Paranjape, S., Adams, S. R., Potter, B. V. L. and Tsien, R. Y. (1991). Cytosolic Ca^{2+} oscillations in REF52 fibroblasts: Ca^{2+}-stimulated IP_3 production or voltage-dependent Ca^{2+} channels as key positive feedback elements. *Cell Calcium* **12**, 153-164.

Jaffe, L. F. (1991). The path of calcium in cytosolic calcium oscillations: A unifying hypothesis. *Proc. Nat. Acad. Sci.USA* **88**, 9883-9887.

Kargacin, G. and Fay, F. S. (1991). Ca^{2+} movement in smooth muscle cells studied with one-and two-dimensional diffusion models. *Biophys J.* **60**, 1088-1100.

Lechleiter, J. and Clapham, D. (1992). Molecular mechanisms of intracellular calcium excitability in *Xenopus laevis* oocytes. *Cell* **69**, 283-294.

Lechleiter, J., Girard, S., Peralta, E. and Clapham, D. (1991). Spiral calcium wave propagation and annihilation in *Xenopus laevis* oocytes. *Science* **252**, 123-126.

Linderman, J. J., Harris, L. J., Slakey, L. L. and Gross, D. J. (1990). Charge-coupled device imaging of rapid calcium transients in cultured arterial smooth muscle cells. *Cell Calcium* **11**, 131-144.

Mahoney, M. G., Randall, C. J., Linderman J. J., Gross, D. J. and Slakey, L. L. (1992). Independent pathways regulate the cytosolic $[Ca^{2+}]$ initial transient and subsequent oscillations in individual cultured arterial smooth muscle cells to extracellular ATP. *Mol. Biol. Cell* **3**, 493-505.

Meyer, T. (1991). Cell signaling by second messenger waves. *Cell* **64**, 675-678.

Meyer, T. and Stryer, L. (1988). Molecular model for receptor-stimulated calcium spiking. *Proc. Nat. Acad. Sci. USA* **85**, 5051-5055.

Miller, D. D., Callaham, D. A., Gross, D. J. and Hepler, P. K. (1992). Free Ca^{2+} gradient in growing pollen tubes of *Lilium*. *J. Cell Sci.* **101**, 7-12.

Moore, E. D. W., Becker, P. L., Fogarty, K. E., Williams, D. A. and Fay, F. S. (1990). Ca^{2+} imaging in single living cells: theoretical and practical issues. *Cell Calcium* **11**, 157-179.

Poenie, M. (1990). Alteration of intracellular Fura-2 fluorescence by viscosity: A simple correction. *Cell Calcium* **11**, 85-91.

Roe, M. W., Lemasters, J. J. and Herman, B. (1990). Assessment of Fura-2 for measurements of cytosolic free calcium. *Cell Calcium* **11**, 63-73.

Rooney, T. A., Sass, E. J., and Thomas, A. P. (1990). Agonist-induced cytosolic calcium oscillations originate from a specific locus in single hepatocytes. *J. Biol. Chem.* **265**, 10792-10796.

Sala, F. and Hernandez-Cruz, A. (1990). Calcium diffusion modeling in a spherical neuron: Relevance of buffering properties. *Biophys. J.* **57,** 313-324.

Somlyo, A. P. and Himpens, B. (1989). Cell calcium and its regulation in smooth muscle. *FASEB J.* **3**, 2266-2276.

Speksnijder, J. E., Miller, A. L., Weisenseel, M. H., Chen, T. H. and Jaffe, L. F. (1989). Calcium buffer injections block fucoid egg development by facilitating calcium diffusion. *Proc. Nat. Acad. Sci. USA* **86**, 6607-6611.

Takamatsu, T. and Wier, W. G. (1990). Calcium waves in mammalian heart: quantification of origin, magnitude, waveform, and velocity. *FASEB J.* **4**, 1519-1525.

Wier, W. G. and Blatter, L. A. (1991). Ca^{2+}-oscillations and Ca^{2+}-waves in mammalian cardiac and vascular smooth muscle cells. *Cell Calcium* **12**, 241-254.

(Received 18 November 1992 - Accepted 13 January 1993)